

On the Semantics of LM Latent Space: A Vocabulary-defined Approach

Jian Gu¹ Chunyang Chen¹ Aldeida Aleti¹

Abstract

Understanding the latent space of language models (LM) is crucial to refining their performance and interpretability. Existing analyses often fall short in providing disentangled (model-centric) insights into LM semantics, and neglect essential aspects of LM adaption. In response, we introduce a pioneering method called vocabulary-defined semantics, which establishes a reference frame within the LM latent space, ensuring disentangled semantic analysis grounded in LM vocabulary. Our approach transcends prior entangled analysis, leveraging LM vocabulary for model-centric insights. Furthermore, we propose a novel technique to compute logits, emphasising differentiability and local isotropy, and introduce a neural clustering module for semantically calibrating data representations during LM adaptation. Through extensive experiments across diverse text understanding datasets, our approach outperforms state-of-the-art methods of retrieval-augmented generation and parameter-efficient finetuning, showcasing its efficacy and broad applicability. Our findings not only shed light on LM mechanics, but also offer practical solutions to enhance LM performance and interpretability.

1. Introduction

With the rapid development of deep learning and generative neural models, the foundational values of large-scale LMs are attracting mass attention for upcoming opportunities and risks (Bommasani et al., 2021). Technically, the opportunities and risks of LMs are greatly affected by the entanglement of LM latent space. The entanglement derives the gap between the machine-friendly features (embeddings, representations, etc) and the human-friendly results (tokens, pixels, etc). The gap determines the performance of neural models and the human confidence of neural models.

Considering the meaning of the latent space analysis to data and models, any potential progress in this direction is important. The latent space is a high-dimensional complex vector space. It can be used to either analyse the characteristics of data or analyse the functionality of neural models, and

further direct the next steps on processing the data or modifying the models. Some illustration or probing techniques connect the latent space to visuals and results, but few interpretations are on the latent space itself (Arvanitidis et al., 2017). In the context of language models, such as natural language processing models represented by transformers, where the analysis in the latent space is mainly on semantics, we explored and concluded a few limitations as follows. In this paper, we also gave our countermeasures.

On one hand, the common perspective of semantic analysis in LM latent space is entangled (data-centric), not disentangled (model-centric). It is meaningful to the data but hard to benefit the model. For example, by checking the scattered shape of data representations in the LM latent space, we may know which training data may be outlier or misleading and why some test data are processed wrongly by the LM. However, it is hard to know, on the given data, how well LMs will perform and how to make LMs perform better.

On the other hand, there are negligences in prior work on two important LM topics: Retrieval-Augmented Generation (RAG) and Parameter-Efficient Finetuning (PEFT). For RAG, the prior work is trying to find the most referenceable data, but the practice tends to introduce deviations, even though it can reduce the deviations in LM inference. For PEFT, the adaptation is centered on fine-tuning the partial but essential parameters in the LM layers. However, the LM-head matrix also matters, and its effects cannot be ignored.

To resolve the above-mentioned issues, in this paper, we propose a novel, intuitive, and effective approach to formulate the semantics of LM latent space: *vocabulary-defined semantics*. In particular, we have the following countermeasures: (1) we define a reference frame in the latent space to realize the disentanglement, namely define its semantic property; (2) we treat the labels in the LM vocabulary as the referenceable data, to avoid deviations of the retrievable data; (3) we use a novel practice to compute the logits, to convert the adaptation of the LM-head matrix (and LM layers) as the refinement of data representations. We will explain these points further in detail in this paper. In addition, we conducted large-scale experiments and detailed analysis across diverse datasets of text understanding, with two families of LLMs. The replication repository is attached as supplementary material. Our contributions are as follows:

- (in concept) we propose a reference frame to analyze the semantics of LM latent space. Compared to prior work of analyzing the semantics from an entangled perspective, our work is a novel disentangled perspective;
- (in theory) we propose a novel way to compute logits, using distance measurement instead of typical matrix multiplication. It is supported by the differentiability and the local isotropy of transformer models;
- (in practice) we propose using a lightweight neural clustering module to calibrate the data representations semantically, for LM adaptation. It equals fine-tuning both the LM-head matrix and LM layers. It outperforms the SOTAs in effectiveness and efficiency.

2. Semantics of LM Latent Space

We introduce concepts of “semantic basis” and “semantic feature” as the precondition to define the semantics of LM latent space. Further, we conduct “semantic calibration” as a practice to leveraging the semantic property: (1) For a given LM, we obtain the corresponding representations of vocabulary labels by solving the pseudoinverse matrix of LM head, and treat such representation as “semantic basis”; (2) Based on the differentiability of neural networks and local isotropy of the latent space of Transformer models, we proposed a hypothesis that, *the distances of a representation with semantic bases indicate its distribution in the vocabulary*. Then, we proposed a novel method to compute logits, that is, taking the distance-based similarities with semantic bases as logits, called “semantic feature”; (3) We regard the LM learning process (such as finetuning) as a clustering problem, where the golden cluster centroids are specified as the semantic bases. Leveraging a high-dimensional transformation to refine the data representations, their semantics are calibrated to the ground truth. We call such a process of representation refinement “semantic calibration”.

Lets demonstrate with an LM, whose vocabulary consists of five colorful labels, as shown in Figure 1: (1) On the semantic basis (see the upper-left), we obtained the semantic bases in the latent space, represented by large color dots. The colors correspond to the labels in the vocabulary one to one; (2) On the semantic feature (see the upper-right), we use a small dark dot to represent a representation from the test set. We compute its similarities with the semantic bases using distance measurement, and then, take the semantic feature as logits. The logits are normalized as distribution in the vocabulary, and the argmax label is *orange*; (3) On the semantic calibration (see the bottom), we use small color dots to represent the representations from the training set, and their color indicates the corresponding ground truth. Originally, the small dots were mixed and scattered all around. Therefore, we learn a transformation to gather them by color,

into clusters centered in the corresponding semantic basis. The calibration is on the whole latent space, affecting the representations from the test set, so the dark dot also moved. We recompute the semantic feature of the dark dot, and see its logits have changed, and the argmax label is now *violet*.

2.1. Semantic Basis

In LM latent space, the semantic similarity between data representations is computed via distance measurement. Besides, the data representation is projected to the LM vocabulary as the logits, and its actual semantic meaning is represented by the distribution and the argmax label. Given this, we propose to use the vocabulary to model the semantics of LM latent space, in the following two steps.

First, we define heuristic logits of disentangled semantic meanings. We take onehot embeddings as the most semantically representative distributions of the vocabulary. Assuming a vocabulary of size v , we need v unique semantic bases to represent v different semantic meanings. Since the softmax operation maintains monotonicity, we can further regard the onehot distributions as onehot logits.

Then, we compute the corresponding representation of the heuristic logits. For a given LM-head matrix, we conduct matrix multiplication to get the corresponding representation in the latent space. Since we compute the representations with the logits and the LM-head, instead of using the LM-head matrix \mathbb{W} , we use its pseudoinverse \mathbb{W}^+ . For every logits, we multiply the heuristic logits \vec{l}_i by the pseudoinverse matrix \mathbb{W}^+ to obtain the corresponding representation \vec{r}_i . The computation is equivalence to treat and solve the least squares problem of a system of linear equations. We call each of the obtained vectors *semantic basis*. The operation is shown in Equation (1).

$$\vec{r} = \vec{l} \cdot \mathbb{W}^+ \quad (1)$$

where \vec{r} and \vec{l} are the representation and the logits, \mathbb{W}^+ is the pseudoinverse of LM-head matrix.

With the semantic bases, we can define a reference frame in the LM latent space. The probability distribution in the vocabulary is disentangled, since each label in the vocabulary represents a unique meaning. In contrast, the data representation is entangled, since the dimension of latent space is much smaller than the size of the vocabulary. The reference frame will be used to realize disentanglement.

2.2. Semantic Feature

For a given representation, we can compute the logits (in a novel way) based on its projection to the semantic bases. In

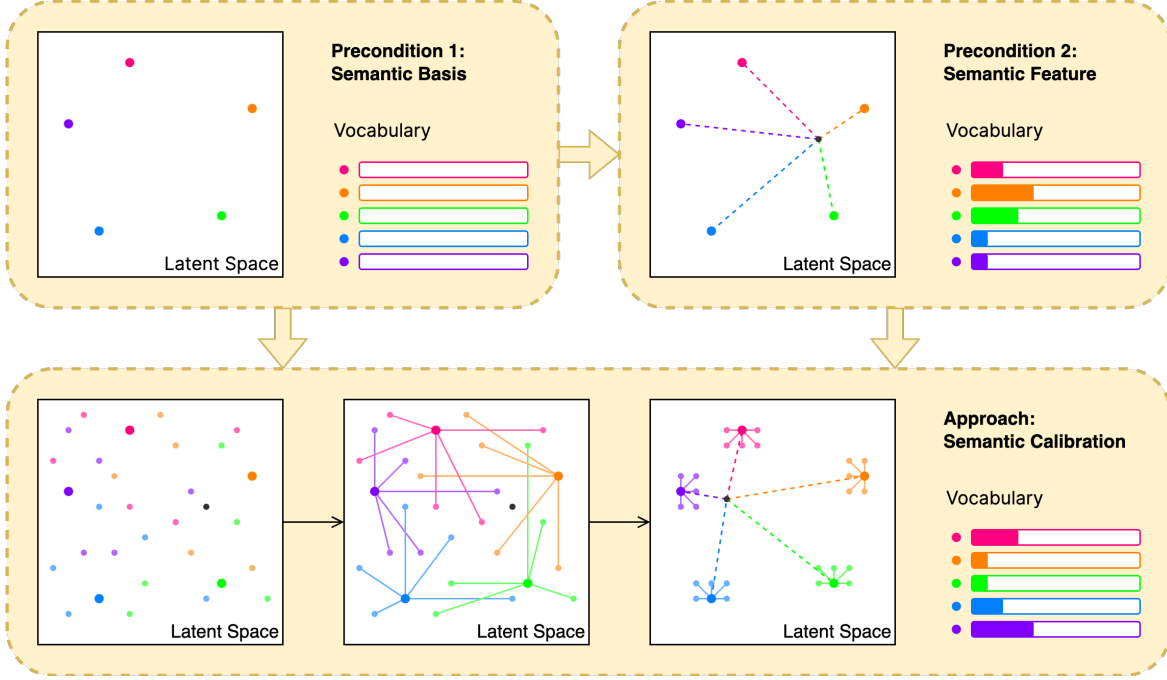


Figure 1. The Illustration of Semantic Basis, Semantic Feature, and Semantic Calibration.

contrast, the typical practice is to multiply the representation with the LM-head matrix.

Due to the natural differentiability of neural networks and the isotropy of Transformer models, we can convert the logits computation from matrix multiplication to distance measurement. If a neural network can be trained with back-propagation, then it is naturally differentiable, since back-propagation requires differentiable neural modules and loss functions (Rumelhart et al., 1986). The differentiability means that, in any direction of a high-dimensional space, infinitesimal increments in the nonlinear function can be approximated by a linear function. Therefore, leveraging the vocabulary-based semantic bases, we can conclude that *if a given last-layer representation in the latent space is close enough to one semantic basis, then its distribution on the vocabulary will also approach the corresponding onehot distribution*. Meanwhile, the latent space of Transformer models is proved as locally isotropic (Cai et al., 2021), in terms of information and semantics. Isotropy means that the properties of a space are uniform in all directions. That is, in different directions of the latent space, the semantic differences of representations in the same distance remain close. Therefore, when we consider all semantic bases, instead of only one basis, the hypothesis is almost true that *the similarity of representations in the latent space remains positively correlated with the similarity of the corresponding distributions on the vocabulary*.

Vocabulary Affinity Inference (VAI). For a given last-layer

representation, the logits are generally obtained by multiplying the LM-head matrix. Leveraging the positive correlation between the representation similarity in the latent space and the distribution similarity on the vocabulary, we compute the logits based on its distance-based similarities with the semantic bases. If it is the cosine distance, then the logits indicate the projection to the semantic bases, which we call *semantic feature*. Further, the logits can be used to compute the probability distribution, as shown in Algorithm 1.

Algorithm 1 Vocabulary Affinity Inference.

Data: n semantic bases \vec{b}_i ; representation \vec{r}
Result: probabilities $probs$ on the vocabulary
 // define logits as 1d-tensor
 1 $logits \leftarrow \text{INIT_1D_TENSOR}(n)$
 // iterate over all semantic bases
 2 **for** $i \leftarrow 0$ **to** $n - 1$ **do**
 // measure the vector distance
 3 $distance \leftarrow \text{DISTANCE_METRIC}(\vec{b}_i, \vec{r})$
 // convert distance to similarity
 4 $similarity \leftarrow \text{DIST_TO_SIMI}(distance)$
 // compose logits with similarities
 5 $logits[i] \leftarrow similarity$
 // convert logits to distribution
 6 $probs \leftarrow \text{SOFTMAX}(logits)$

In a reference frame, vocabulary affinity inference is needed. It will be used to compute the semantic feature for each

representation. The semantic feature is a disentanglement to the corresponding representation, since VAI is equivalent to the typical matrix multiplication for logits computation.

2.3. Semantic Calibration

Based on the concepts of semantic basis and semantic feature, we formulate the semantic property of LM latent space with a reference frame and a distance-based way for logits computation. Further, we can define LM adaptation as a process of calibrating the semantics of the given data.

For an LM latent space scattered with data representations, the typical LM adaptation process can be realized by *clustering* them centered on the corresponding semantic bases. In our approach, we specify each semantic basis as the oracle centroid of each cluster. In the optimal situation of LM adaptation, the last-layer representations of the same semantic meaning, namely corresponding to the same label, should gather in the same cluster. We will use a learning-based method for the centroid-specified clustering. We call the process *semantic calibration*.

We inject a neural clustering module into the LM for the process of semantic calibration. The clustering module consists of a multi-layer perceptron (MLP), a channel attention (CA), and a layer normalization (LN), as shown in Equation (2). The channel attention learns the coefficients of the representations, based on the information in the channel domain (Hu et al., 2017), as shown in Equation (3). The coefficients are a sum of the Bottleneck (Bn) outputs, respectively on the average-pooling (avg) and the maximum-pooling (max) of the representations. While the perceptron and normalization learn a non-linear transformation in the latent space.

$$\lambda(\vec{r}) = \text{LN}(\text{MLP}(\text{CA}(\vec{r}))) \quad (2)$$

$$\text{CA}(\vec{r}) = \vec{r} \odot (\text{Bn}(\text{avg}(\vec{r})) + \text{Bn}(\text{max}(\vec{r}))) \quad (3)$$

In module training, the logits are computed with the ground truth using VAI to obtain the loss, such as the cross-entropy loss. In module inference, the logits are processed by a softmax function to get the distribution on the vocabulary.

3. Experiments

In the following, we first introduce the experimental setup, and then analyze the results on the effectiveness and efficiency. We conduct the experiments on diverse datasets and a wide range of GPT2 and Pythia scales. In the results, the optimal scores are stressed with the gray color, and our approach (the second column) is stressed in bold.

Table 1. Stats of Datasets, and Number of Allowed Shots.

		AGNews	CARER	MR	MRPC	SST5	SUBJ	TREC	WebSS
# of Classes		4	6	2	2	5	2	6	8
Is Balanced		✓	✗	✓	✗	✗	✓	✗	✗
Average Length of Prompts		59.2	26.1	31.9	63.2	29.0	34.1	16.4	29.9
Num. of Data	Train	120,000	16,000	8,662	4,076	8,544	8,000	5,452	10,060
	Test	7,600	2,000	2,000	1,725	2,210	2,000	500	2,280
Num. of Shots	1k-context	2	4	8	4	4	8	8	2
	2k-context	4	8	16	8	8	16	16	4

Table 2. Stats of GPT2 and Pythia Models.

	GPT2					Pythia				
	Small	Medium	Large	XL	XS	Small	Medium	Large	XL	XXL
Parameters	117M	345M	762M	1.5B	70M	160M	410M	1.0B	1.4B	2.8B
Num. of Layer	12	24	36	48	6	12	24	16	24	32
Dimension Size	768	1024	1280	1600	512	768	1024	2048	2048	2560

3.1. Setup

Datasets. We use 8 established text understanding datasets, respectively for binary classification and multiclass classification. For the binary case, the datasets are MR (Pang & Lee, 2005), MRPC (Dolan & Brockett, 2005), and SUBJ (Pang & Lee, 2004). For the multiclass case, the datasets are AG-News (Zhang et al., 2015), CARER (Saravia et al., 2018), SST5 (Socher et al., 2013), TREC (Voorhees & Tice, 2000), and WebSS (Phan et al., 2008). In the experiments, we use few-shot learning with prompt templates (see Appendix D), making full use of the LM context length. The statistics of datasets are shown in Table 1.

Models. We use strong and recognized open-source LLMs and involve two LLM families in our experiments, one is the GPT2 series (117M-1.5B) (Radford et al., 2019), and the other one is the Pythia (Biderman et al., 2023) series (70M-2.8B). The details are available in Table 2.

Baselines. In our experiments, we study the effects of semantic calibration on general In-Context Learning, short as ICL (Min et al., 2022). Besides, we compare with the SOTA retrieval-augmented method, Knn Prompting, short as KP (Xu et al., 2023). We reproduce the practice of ICL and KP in the KP paper (Xu et al., 2023) as the baseline. In addition, we also compare with parameter-efficient fine-tuning methods, including LORA (Hu et al., 2021) and IA³ (Liu et al., 2022), as an extension of the study, considering our practice involves an additional neural module.

Metrics. On the metrics, we mainly take *Accuracy* to measure the prediction quality.

3.2. Pipelines

On ICL, we retrieve the demonstrations randomly from the training set, and take the same number of demos for each class, making the full usage of the allowed context length.

On KP, the practice is roughly the same, but the retrieval process is led by the KL divergence. The data similar in the

Table 3. Accuracy on Text Understanding with GPT2 Models.

GPT2	Method	AGNews	CARER	MR	MRPC	SST5	SUBJ	TREC	WebSS	AVG
Small	ICL	0.283	0.372	0.558	0.665	0.309	0.500	0.552	0.315	0.444
	KP	0.860	0.373	0.706	0.559	0.305	0.842	0.810	0.740	0.649
	LoRA	0.618	0.395	0.553	0.665	0.315	0.500	0.548	0.324	0.490
	IA ³	0.376	0.400	0.554	0.665	0.326	0.500	0.548	0.322	0.461
	SC	0.904	0.633	0.816	0.672	0.459	0.870	0.930	0.749	0.754
Medium	ICL	0.545	0.348	0.534	0.665	0.157	0.533	0.546	0.313	0.455
	KP	0.852	0.343	0.742	0.587	0.357	0.878	0.818	0.776	0.669
	LoRA	0.828	0.348	0.535	0.665	0.162	0.531	0.544	0.325	0.492
	IA ³	0.673	0.348	0.534	0.665	0.161	0.529	0.548	0.334	0.474
	SC	0.927	0.645	0.838	0.682	0.511	0.941	0.940	0.836	0.790
Large	ICL	0.684	0.441	0.793	0.665	0.286	0.617	0.622	0.208	0.539
	KP	0.854	0.394	0.847	0.597	0.375	0.895	0.882	0.763	0.701
	LoRA	0.886	0.449	0.862	0.665	0.281	0.732	0.634	0.340	0.606
	IA ³	0.824	0.452	0.842	0.665	0.280	0.693	0.632	0.268	0.582
	SC	0.926	0.667	0.888	0.729	0.526	0.959	0.964	0.814	0.809
XL	ICL	0.709	0.292	0.567	0.665	0.193	0.527	0.586	0.266	0.475
	KP	0.884	0.397	0.803	0.588	0.381	0.901	0.854	0.791	0.700
	LoRA	0.891	0.484	0.767	0.665	0.188	0.666	0.608	0.368	0.579
	IA ³	0.831	0.309	0.670	0.665	0.190	0.578	0.594	0.314	0.519
	SC	0.937	0.666	0.879	0.728	0.538	0.959	0.958	0.813	0.809

probability distribution are more likely to be retrieved.

On PEFT methods, we specify the recommended modules be trainable based on their papers (that is, QKV matrices in LoRA, and QKV matrices plus the second FC layer in IA³), using the default hyperparameters (see Appendix A).

In our approach SC, we freeze all LM parameters to merely train the neural clustering module on the training set.

3.3. Effectiveness Study

Compared to SOTA methods, semantic calibration is competitive. It outperforms others in almost all data and models.

Based on the results shown in Table 3, on GPT2 models, SC obtained the optimal average performance, and KP takes the suboptimal position, and then LoRA and IA³. Besides, semantic calibration can usually improve the performance of ICL significantly, and outperform SOTA methods.

The effects of SC to ICL are beneficial and obvious, even though the degree of improvement is dependent on the actual data and model. Compared to different datasets, the improvements of SC are the least on MRPC, and are most obvious on AGNews and WebSS. Considering the number of classes is 2 in MRPC but 4 and 8 in AGNews and WebSS, SC have more effects when the number of classes is larger.

It is noticeable to see both SC and KP outperform PEFT methods. The reason is that, when adapting LMs to the downstream data, the typical finetuning practices tend to ignore the effects of the LM-head matrix. Different from the trainable LM layers, the LM-head matrix represents a perspective of the whole LM latent space. If the matrix stays unchanged, the LM adaption in semantics is limited. KP picks the demonstrations based on the logits, so can partially have the effects of finetuning the LM-head matrix, but also introduce unexpected deviations. In contrast, SC is a disentanglement process, since it uses the reference frame as the perspective. By optimizing the data representations, SC realizes finetuning the LM-head matrix equivalently.

Table 4. Accuracy on Text Understanding with Pythia Models.

Pythia	Method	AGNews	CARER	MR	MRPC	SST5	SUBJ	TREC	WebSS	AVG
XS	ICL	0.350	0.197	0.500	0.665	0.269	0.559	0.422	0.382	0.418
	KP	0.250	0.291	0.500	0.335	0.286	0.500	0.226	0.132	0.315
	LoRA	0.351	0.197	0.500	0.665	0.269	0.559	0.422	0.382	0.418
	IA ³	0.351	0.197	0.500	0.665	0.269	0.559	0.422	0.382	0.418
	SC	0.845	0.561	0.500	0.665	0.357	0.500	0.798	0.556	0.598
Small	ICL	0.517	0.342	0.548	0.665	0.239	0.524	0.360	0.181	0.422
	KP	0.250	0.291	0.500	0.335	0.286	0.500	0.226	0.132	0.315
	LoRA	0.516	0.342	0.547	0.665	0.239	0.524	0.360	0.181	0.422
	IA ³	0.516	0.342	0.547	0.665	0.239	0.524	0.360	0.181	0.422
	SC	0.851	0.565	0.500	0.665	0.443	0.500	0.866	0.562	0.619
Medium	ICL	0.633	0.362	0.806	0.665	0.347	0.689	0.654	0.432	0.573
	KP	0.855	0.532	0.815	0.541	0.375	0.856	0.836	0.776	0.698
	LoRA	0.617	0.356	0.813	0.665	0.326	0.686	0.654	0.468	0.573
	IA ³	0.604	0.370	0.803	0.665	0.331	0.688	0.650	0.433	0.568
	SC	0.932	0.742	0.859	0.708	0.496	0.943	0.940	0.804	0.803
Large	ICL	0.612	0.352	0.537	0.665	0.340	0.662	0.732	0.492	0.549
	KP	0.877	0.559	0.857	0.583	0.395	0.883	0.880	0.801	0.729
	LoRA	0.886	0.578	0.775	0.665	0.381	0.865	0.752	0.495	0.675
	IA ³	0.820	0.419	0.586	0.665	0.351	0.774	0.744	0.494	0.606
	SC	0.936	0.751	0.888	0.734	0.489	0.951	0.962	0.822	0.816
XL	ICL	0.641	0.401	0.844	0.665	0.349	0.602	0.564	0.514	0.572
	KP	0.876	0.557	0.859	0.565	0.435	0.894	0.888	0.807	0.735
	LoRA	0.840	0.552	0.743	0.665	0.354	0.727	0.542	0.513	0.617
	IA ³	0.818	0.442	0.810	0.665	0.358	0.653	0.554	0.514	0.602
	SC	0.938	0.762	0.902	0.715	0.530	0.962	0.958	0.820	0.823
XXL	ICL	0.750	0.260	0.851	0.665	0.483	0.906	0.722	0.496	0.641
	KP	0.881	0.526	0.865	0.574	0.423	0.919	0.844	0.805	0.730
	LoRA	0.888	0.582	0.895	0.665	0.529	0.914	0.768	0.493	0.717
	IA ³	0.848	0.319	0.873	0.665	0.508	0.910	0.734	0.494	0.669
	SC	0.939	0.749	0.901	0.752	0.531	0.956	0.968	0.841	0.830

Based on the results shown in Table 4, on Pythia models, the findings are similar: SC obtained the optimal average performance on all datasets. On medium or larger LMs, KP takes the suboptimal position, and then PEFT methods.

On most datasets, our findings are identical to those on the GPT2 models. However, the situation is a bit special on the MR, MRPC, and SUBJ datasets. The performance of SOTA methods seems different on small-scale models, namely Pythia-XS and Pythia-Small, compared to the cases where it is on larger models. In detail, the performances of all methods almost remain unchanged, and also, their performance is close to, and even the same as each other. By checking the statistics of datasets, we find the three datasets are for binary classification and have merely two different labels. Considering that LM capability is decided by the quality of the last-layer representations, and small-scale models are not that strong, we believe this phenomenon is the result of the joint action of both reasons: the low-quality representations and the binary label space.

Overall, semantic calibration shows advantages in performance and can be a strong measurement to improve the LM capability, especially on medium or larger models, or on complex data (such as a non-binary label space).

3.4. Efficiency Study

Compared to SOTA methods, semantic calibration is strong in efficiency, especially in storage and computation costs.

The clustering module is lightweight and the time cost is small. For a given LM, assume its dimension size of latent representations is d , then the number of trainable parameters consists of $4 * d * d$ for the MLP and $\frac{1}{8} * d * d$ for the Bn.

Assume the size of LM vocabulary is v , and the number of actually-used LM labels is \bar{v} , so the time in the logits computation can be reduced to \bar{v}/v . It indicates an obvious speedup, and is caused by the VAI in logits computation.

On the storage cost, let's say a corpus means a collection of data to retrieve, then KP requires the most in the storage cost, while PEFT methods and SC have much lower costs. As a common practice in LM inference, it is used by all methods in our experiments, so we exclude it from the cost consideration. ICL has no additional storage. In contrast, KP needs to store the probability distribution of a balanced subset of the corpus, that is, $k * v * v$ when the number of nearest neighbors is k . As PEFT methods, LORA and IA³ store the trainable parameters. Taking their recommended setups, the amount of their parameters are $4 * r * d * l$ and $7 * d * l$, when the low-rank parameter is r and the number of LM layers is l . For our approach SC, the storage cost is the neural clustering module, that is, $\frac{33}{8} * d * d$. It can be further reduced to $\frac{33}{8} * d$ via parameterized hypercomplex multiplication (Zhang et al., 2021).

On the computation cost, PEFT methods require the most cost, then SC, while KP requires the least. Since the LM inference is required by all methods, we exclude it from the cost consideration. ICL has no additional computation. In contrast, KP needs to run a forward-pass with the corpus data to obtain the probability distribution. As PEFT methods, LORA and IA³ run both forward-pass and backward-pass on the LM (for each finetuning epoch), even though only updating the partial parameters. For our approach SC, the computation cost includes a forward-pass on the LM, both forward-pass and backward-pass on the neural clustering module (for each calibration epoch), and a computation to solve the pseudoinverse matrix. For example, running GPT2-XL on AGNews with A100, SC costs 27.7 hours in forward-pass and 0.3 hours in semantic calibration, while LORA costs 40.2 hours and IA3 costs 41.6 hours.

4. Analysis and Explanation

In the following, we give a further analysis of the related aspects of our approach, with GPT2-XL and Pythia-XL for the experiments. In the results, the optimal scores are stressed with the gray base color, and our approach (the second column) is highlighted in bold.

4.1. More Study on Vocabulary Affinity Inference

To study the effects of vocabulary affinity inference, we do an ablation study on semantic calibration. The variants take different practices in the logits computation, respectively in training or inference. In the training stage, SC uses VAI for the loss, so we prepare a variant to compute the loss by the matrix multiplication, and mark it with SC[loss]. In

Table 5. Accuracy of Ablation Study with GPT Models.

GPT2	Variant	AGNews	CARER	MR	MRPC	SST5	SUBJ	TREC	WebSS	AVG
Small	SC	0.904	0.633	0.816	0.672	0.459	0.870	0.930	0.749	0.754
	SC[gen]	0.907	0.602	0.817	0.705	0.467	0.932	0.908	0.776	0.764
	SC[loss]	0.250	0.348	0.500	0.665	0.181	0.500	0.162	0.132	0.342
Medium	SC	0.927	0.645	0.838	0.682	0.511	0.941	0.940	0.836	0.790
	SC[gen]	0.928	0.645	0.837	0.690	0.485	0.942	0.942	0.836	0.788
	SC[loss]	0.250	0.348	0.500	0.665	0.231	0.500	0.162	0.132	0.348
Large	SC	0.926	0.667	0.888	0.729	0.526	0.959	0.964	0.814	0.809
	SC[gen]	0.926	0.665	0.888	0.730	0.529	0.959	0.964	0.811	0.809
	SC[loss]	0.250	0.291	0.500	0.665	0.231	0.500	0.226	0.132	0.349
XL	SC	0.937	0.666	0.879	0.728	0.538	0.959	0.958	0.813	0.809
	SC[gen]	0.937	0.668	0.879	0.728	0.539	0.959	0.960	0.815	0.810
	SC[loss]	0.250	0.348	0.500	0.665	0.231	0.500	0.226	0.132	0.356

Table 6. Accuracy of Ablation Study with Pythia Models.

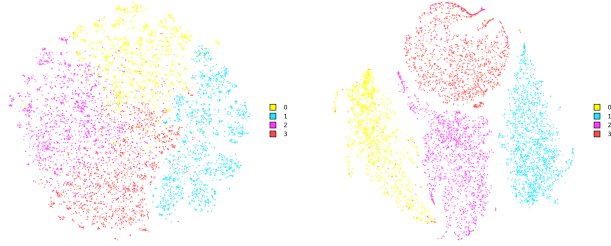
Pythia	Method	AGNews	CARER	MR	MRPC	SST5	SUBJ	TREC	WebSS	AVG
XS	SC	0.845	0.561	0.500	0.665	0.357	0.500	0.798	0.556	0.598
	SC[gen]	0.845	0.566	0.500	0.665	0.355	0.500	0.794	0.594	0.602
	SC[loss]	0.250	0.348	0.500	0.665	0.231	0.500	0.188	0.132	0.352
Small	SC	0.851	0.565	0.500	0.665	0.443	0.500	0.866	0.562	0.619
	SC[gen]	0.851	0.575	0.500	0.665	0.446	0.500	0.864	0.556	0.620
	SC[loss]	0.250	0.348	0.500	0.665	0.364	0.500	0.276	0.132	0.379
Medium	SC	0.932	0.742	0.859	0.708	0.496	0.943	0.940	0.804	0.803
	SC[gen]	0.932	0.742	0.859	0.707	0.495	0.943	0.940	0.806	0.803
	SC[loss]	0.688	0.348	0.858	0.699	0.459	0.932	0.226	0.132	0.542
Large	SC	0.936	0.751	0.888	0.734	0.489	0.951	0.962	0.822	0.816
	SC[gen]	0.936	0.750	0.888	0.734	0.489	0.951	0.962	0.823	0.816
	SC[loss]	0.250	0.348	0.500	0.665	0.476	0.500	0.788	0.132	0.457
XL	SC	0.938	0.762	0.902	0.715	0.530	0.962	0.958	0.820	0.823
	SC[gen]	0.938	0.760	0.902	0.715	0.530	0.962	0.956	0.821	0.823
	SC[loss]	0.696	0.581	0.500	0.665	0.485	0.500	0.946	0.132	0.563
XXL	SC	0.939	0.749	0.901	0.752	0.531	0.956	0.968	0.841	0.830
	SC[gen]	0.940	0.749	0.901	0.752	0.532	0.956	0.968	0.843	0.830
	SC[loss]	0.939	0.348	0.500	0.665	0.286	0.500	0.784	0.132	0.519

the inference stage, SC uses VAI for the generation, so we prepare a variant to compute the generation by the matrix multiplication and mark it with SC[gen].

Based on the results shown in Table 5 and Table 6, compared to our approach SC, SC[gen] has a similar performance while SC[loss] perform much worse. First, the minor difference in the performance of SC and SC[gen] indicates the roughly equivalent effects between the two ways of logits computation, especially when we compare their average scores. It proves the correctness of our hypothesis on the correlations of the representations similarity and distribution similarity. Second, the huge difference in the performance of SC and SC[loss] indicates that it is necessary to use VAI to compute the logits, when training an additional module to the LM. In datasets of binary classification (MR, MRPC, and SUBJ), the performance of SC[loss] is not that bad, especially on the medium or smaller Pythia models.

On the equivalence of two ways to compute the distribution, we also check the case where the logits in both training and inference are computed by matrix multiplication, and its results are identical to SC[loss]. In contrast, the performance difference between SC and SC[gen] is small, but SC[gen] is slightly better. The difference may be caused by the numeric precision error in the conversion from the distribution to the representation, in computing the pseudoinverse matrix. Since VAI is used to obtain the loss, the numeric precision error will not affect SC[loss], but does affect SC.

On the necessity of VAI in training the additional neural



(a) AGNews Test Set w/o SC (b) AGNews Test Set w/ SC

Figure 2. Semantic Calibration (tSNE) in GPT2-XL Latent Space.

module, we conclude it as an operation of semantic disentanglement. Based on the hypothesis on the correlations of the representations similarity and distribution similarity, no matter which way is used to compute logits, we expect the distribution on the vocabulary to be close to the corresponding onehot distribution, therefore, the representation in the latent space be close to the corresponding semantic basis. In the typical matrix multiplication way to compute logits, the computation is between the representation and the LM-head matrix, so each data is optimized with the pretrained knowledge of all labels in the vocabulary. In contrast, in the distance measurement way, the computation is only between the representation and the corresponding semantic basis.

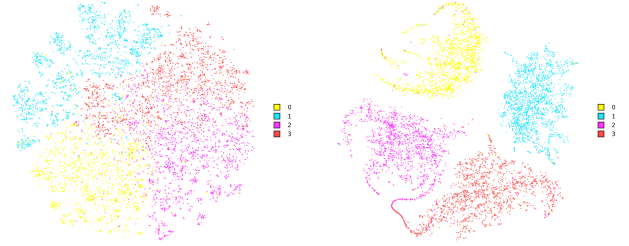
If we say, the LM-head matrix represents a semantical perspective, then for each data, the matrix multiplication way lets the optimization target be close to the probability of all labels (learned in the LM pretraining process), or the estimated confidence level in the LM perspective. While the distance measurement way lets the optimization target be close to the ground truth, since we explicitly specify the semantic basis for each data to transform the representation.

Further, we believe the adaptation of the LM-head matrix has been ignored for a long time. Even though finetuning LM to adapt the downstream data or tasks is common, to the best of our knowledge, there is no work centered on the adaptation of the LM-head matrix. Instead of directly adapting the LM perspective, VAI applies semantic disentanglement on the LM-head matrix to obtain a semantic basis, and then avoids using the matrix in the logits computation.

4.2. More Study on Semantic Calibration

To illustrate the effects of semantic calibration, we visualize representations in the latent space using tSNE (Arvanitidis et al., 2017). As shown in Figure 2 and Figure 3, before semantic calibration, the data representations were messily scattered. In contrast, after semantic calibration, the representations scatter into a few clusters, and in each cluster, the representations correspond to the same semantic meaning.

Since the clustering quality is promoted by semantic calibra-



(a) AGNews Test Set w/o SC (b) AGNews Test Set w/ SC

Figure 3. Semantic Calibration (tSNE) in Pythia-XL Latent Space.

 Table 7. Accuracy with k Nearest-Neighbor Methods.

Dataset	Param	GPT2					Pythia				
		Small	Medium	Large	XL	XS	Small	Medium	Large	XL	XXL
AGNews	$k=1$ [w/o]	0.672	0.701	0.768	0.792	0.602	0.675	0.787	0.792	0.798	0.802
	$k=1$ [w/]	0.903	0.917	0.919	0.935	0.796	0.805	0.922	0.935	0.937	0.939
	$k=16$ [w/o]	0.794	0.807	0.852	0.876	0.748	0.811	0.856	0.879	0.876	0.880
	$k=16$ [w/]	0.910	0.928	0.926	0.937	0.854	0.863	0.932	0.936	0.938	0.940
	$k=256$ [w/o]	0.822	0.835	0.864	0.886	0.777	0.839	0.865	0.890	0.886	0.888
	$k=256$ [w/]	0.910	0.929	0.926	0.937	0.857	0.870	0.932	0.936	0.938	0.940
WebSS	$k=1$ [w/o]	0.187	0.248	0.240	0.262	0.232	0.243	0.354	0.318	0.343	0.375
	$k=1$ [w/]	0.595	0.644	0.658	0.685	0.313	0.358	0.663	0.688	0.686	0.707
	$k=16$ [w/o]	0.238	0.323	0.390	0.421	0.362	0.384	0.563	0.517	0.521	0.562
	$k=16$ [w/]	0.651	0.693	0.668	0.687	0.410	0.462	0.668	0.689	0.687	0.707
	$k=256$ [w/o]	0.300	0.439	0.532	0.596	0.503	0.512	0.679	0.691	0.676	0.696
	$k=256$ [w/]	0.693	0.782	0.750	0.769	0.537	0.566	0.751	0.748	0.737	0.742

tion (see Appendix B and Appendix C). We can anticipate that, for retrieval-augmented methods, the performance will also benefit from semantic calibration.

For ease of description, we use “sibling” to describe data representations that correspond to the same label in the vocabulary, and use “neighbor” to describe data representations that are close to each other in latent space. In the process of semantic calibration, for each data, its siblings are gradually becoming its neighbors.

We experimented with semantic calibration to validate its effects on nearest-neighbor methods, that is, predicting the class of data representations with the reference to the nearest neighboring data in the latent space. As shown in Table 7, there are obvious improvements in the performance when we apply the semantic calibration. When the neighboring number k increased from $k = 1$ to $k = 256$, the performance of [w/o] is gradually increased and becomes closer to that of [w/]. The accuracy changes shown on [w/o] mean, that semantic calibration transforms the representations to make more neighboring data be the sibling data.

5. Related Work

Generally, retrieval-augmented methods combine data retrieval and LM for better performance, such as in-context learning, which prompts LM with the retrieved task demonstrations. The demonstrations are in the form of an input-output pair, and will compose with the given input as the new input. The retrieval is conducted based on the similarity

of the corpus data to the given input. Similarly, the data to retrieve can be the context with the potentially related background. The general practice of similarity measurement in data retrieval is based on embeddings or representations, but KP evaluates the similarities of data based on the logits. Besides, KP retrieval the same amount of data for each label in the vocabulary for balance. Similar to retrieval-augmented methods, *nearest-neighbor methods* use the retrieval technique for improvements as well. However, it happens at the output side, such as the LM last-layer, instead of the input side. The data to retrieve is key-value pairs, for example, let the representation be the key and the corresponding ground truth be the value. The given representation is used as the query to retrieve the related history data. Then LM does inference with hybrid logits: one is from the model prediction while the other one is from the nearest-neighbor retrieval. The hybrid logits will be used to compute a normalized probability distribution. It has been used for language modeling in k NN-LM (Khandelwal et al., 2020) and machine translation in k NN-MT (Khandelwal et al., 2021). A similar practice is using activations as the key (Grave et al., 2017).

To reduce the computation cost of finetuning large-scale LMs, and the storage cost of the finetuned models, PEFT methods are proposed. They only update partial parameters. Besides, compared with fully finetuning, PEFT methods can better avoid catastrophic forgetting (Goodfellow et al., 2013), and learn better from a small amount of data. Adapter methods directly introduce new modules to the LMs, such as bottleneck adapters (Houlsby et al., 2019) and compacter (Davison, 2021). PROMPT TUNING prepends tunable tokens to the input data. Similarly, PREFIX-TUNING modifies the multi-head attention with new parameters, that is, prepending trainable vectors to the key and value matrices. Besides, LORA (Hu et al., 2021) uses a low-rank matrix to learn the updates on the self-attention weight matrix. While IA³ (Liu et al., 2022) rescales the activations by tuning additional vectors. In addition, some work is the combinations of other PEFT methods (Mao et al., 2021). For example, mix-and-match adapters are a combination of prefix-tuning and bottleneck adapters (He et al., 2021).

6. Discussion

In this paper, we defined and explored the semantic property of the latent space, especially on the LM last-layer. However, our practice can be extended to all LM layers, not merely the LM last-layer. We believe the utilization of LM semantic property can benefit the upcoming work in model training, or potentially model verification.

Considering the semantic basis is based on the vocabulary, we can therefore duplicate the practice on the LM last-layer to the LM first-layer as well. For the sake of the opposite computation direction of representation, the semantic basis

can be obtained by a matrix multiplication between onehot embedding and the embedding matrix.

For layers between LM first-layer and last-layer, the vocabulary cannot be directly used to build the reference frame. We follow the principle of Occam’s razor, that is, taking the simplest explanation for an observation is most likely to be correct. We take a hypothesis that, *on the semantic property of a given LM, the latent spaces of neighboring LM layers should be similar. If not the same, the changes should be smooth and simple*. It also affects the reference frame (semantic basis). In this way, we extend the applicability of vocabulary-defined semantics to all LM layers.

Depending on whether the embedding matrix and the LM-head matrix are shared, there are two situations: If shared, such as in Transformer (Vaswani et al., 2017), then the reference frame in the LM last-layer is the same as the LM first-layer. We call this case “static latent space”, since the reference frame tends to keep stable in all LM layers. We can assume all middle layers have the same reference frame. If not shared, such as in LLaMA (Touvron et al., 2023), then the reference frame in the LM last-layer is different from the LM first-layer. We call this case “dynamic latent space”, since the reference frame is changing when moving across different layers. We may use interpolation methods to estimate the reference frame of the middle layers.

7. Conclusion

In this paper, we proposed the concepts of semantic basis and semantic feature to define the semantic property of LM latent space. It indicates the definition of a reference frame, and a distance-based way for logits computation. Further, we proposed semantic calibration for LM adaption.

As a whole, the definition of semantic property realized the disentanglement in LM latent space. It may be extremely useful for model training, such as LM finetuning. Besides, it benefits other tasks where the ground truth is used to supervise the latent representation, such as model verification.

Based on our results, semantic calibration can greatly improve the LM performance in text understanding tasks. It also outperforms prior work in RAG and PEFT. Meanwhile, semantic calibration is meaningful to nearest-neighbor methods, which may further benefit neuro-symbolic methods.

In future work, we will introduce the semantic property into the training process of LMs, or the finetuning work of all LM layers instead of merely the LM last-layer. In addition, we will do more experiments based on the theory of vocabulary-defined semantics. On one hand, studying the actual semantic situation of representations in the LM layers; On the other hand, studying the potential association between the representations and the semantic bases.

References

- Arvanitidis, G., Hansen, L. K., and Hauberg, S. Latent space oddity: on the curvature of deep generative models. *arXiv: Machine Learning*, 2017. URL <https://api.semanticscholar.org/CorpusID:51780574>.
- Biderman, S., Schoelkopf, H., Anthony, Q. G., Bradley, H., O’Brien, K., Hallahan, E., Khan, M. A., Purohit, S., Prashanth, U. S., Raff, E., Skowron, A., Sutawika, L., and van der Wal, O. Pythia: A suite for analyzing large language models across training and scaling. *ArXiv*, abs/2304.01373, 2023. URL <https://api.semanticscholar.org/CorpusID:257921893>.
- Bommasani, R., Hudson, D. A., Adeli, E., Altman, R., Arora, S., von Arx, S., Bernstein, M. S., Bohg, J., Bosse-lut, A., Brunskill, E., Brynjolfsson, E., Buch, S., Card, D., Castellon, R., Chatterji, N. S., Chen, A. S., Creel, K. A., Davis, J., Demszy, D., Donahue, C., Doumbouya, M., Durmus, E., Ermon, S., Etchemendy, J., Ethayarajh, K., Fei-Fei, L., Finn, C., Gale, T., Gillespie, L., Goel, K., Goodman, N. D., Grossman, S., Guha, N., Hashimoto, T., Henderson, P., Hewitt, J., Ho, D. E., Hong, J., Hsu, K., Huang, J., Icard, T. F., Jain, S., Jurafsky, D., Kalluri, P., Karamcheti, S., Keeling, G., Khani, F., Khattab, O., Koh, P. W., Krass, M. S., Krishna, R., Kuditipudi, R., Kumar, A., Ladhak, F., Lee, M., Lee, T., Leskovec, J., Levent, I., Li, X. L., Li, X., Ma, T., Malik, A., Manning, C. D., Mirchandani, S., Mitchell, E., Munyikwa, Z., Nair, S., Narayan, A., Narayanan, D., Newman, B., Nie, A., Niebles, J. C., Nilforoshan, H., Nyarko, J. F., Ogut, G., Orr, L. J., Papadimitriou, I., Park, J. S., Piech, C., Portelance, E., Potts, C., Raghunathan, A., Reich, R., Ren, H., Rong, F., Roohani, Y. H., Ruiz, C., Ryan, J., R’e, C., Sadigh, D., Sagawa, S., Santhanam, K., Shih, A., Srinivasan, K. P., Tamkin, A., Taori, R., Thomas, A. W., Tramèr, F., Wang, R. E., Wang, W., Wu, B., Wu, J., Wu, Y., Xie, S. M., Yasunaga, M., You, J., Zaharia, M. A., Zhang, M., Zhang, T., Zhang, X., Zhang, Y., Zheng, L., Zhou, K., and Liang, P. On the opportunities and risks of foundation models. *ArXiv*, abs/2108.07258, 2021. URL <https://api.semanticscholar.org/CorpusID:237091588>.
- Cai, X., Huang, J., Bian, Y.-L., and Church, K. W. Isotropy in the contextual embedding space: Clusters and manifolds. In *International Conference on Learning Representations*, 2021. URL <https://api.semanticscholar.org/CorpusID:235614342>.
- Davison, J. Compacter: Efficient low-rank hypercomplex adapter layers. In *Neural Information Processing Systems*, 2021. URL <https://api.semanticscholar.org/CorpusID:235356070>.
- Dettmers, T., Pagnoni, A., Holtzman, A., and Zettlemoyer, L. Qlora: Efficient finetuning of quantized llms. *ArXiv*, abs/2305.14314, 2023. URL <https://api.semanticscholar.org/CorpusID:258841328>.
- Dolan, W. B. and Brockett, C. Automatically constructing a corpus of sentential paraphrases. In *International Joint Conference on Natural Language Processing*, 2005. URL <https://api.semanticscholar.org/CorpusID:16639476>.
- Goodfellow, I. J., Mirza, M., Da, X., Courville, A. C., and Bengio, Y. An empirical investigation of catastrophic forgetting in gradient-based neural networks. *CoRR*, abs/1312.6211, 2013. URL <https://api.semanticscholar.org/CorpusID:12730344>.
- Grave, E., Joulin, A., and Usunier, N. Improving neural language models with a continuous cache. *ArXiv*, abs/1612.04426, 2017.
- He, J., Zhou, C., Ma, X., Berg-Kirkpatrick, T., and Neubig, G. Towards a unified view of parameter-efficient transfer learning. *ArXiv*, abs/2110.04366, 2021. URL <https://api.semanticscholar.org/CorpusID:238583580>.
- Houlsby, N., Giurghi, A., Jastrzebski, S., Morrone, B., de Laroussilhe, Q., Gesmundo, A., Attariyan, M., and Gelly, S. Parameter-efficient transfer learning for nlp. *ArXiv*, abs/1902.00751, 2019. URL <https://api.semanticscholar.org/CorpusID:59599816>.
- Hu, J., Shen, L., Albanie, S., Sun, G., and Wu, E. Squeeze-and-excitation networks. *2018 IEEE/CVF Conference on Computer Vision and Pattern Recognition*, pp. 7132–7141, 2017. URL <https://api.semanticscholar.org/CorpusID:140309863>.
- Hu, J. E., Shen, Y., Wallis, P., Allen-Zhu, Z., Li, Y., Wang, S., and Chen, W. Lora: Low-rank adaptation of large language models. *ArXiv*, abs/2106.09685, 2021. URL <https://api.semanticscholar.org/CorpusID:235458009>.
- Khandelwal, U., Levy, O., Jurafsky, D., Zettlemoyer, L., and Lewis, M. Generalization through memorization: Nearest neighbor language models. *ArXiv*, abs/1911.00172, 2020.
- Khandelwal, U., Fan, A., Jurafsky, D., Zettlemoyer, L., and Lewis, M. Nearest neighbor machine translation. *ArXiv*, abs/2010.00710, 2021.

- Liu, H., Tam, D., Muqeeth, M., Mohta, J., Huang, T., Bansal, M., and Raffel, C. Few-shot parameter-efficient fine-tuning is better and cheaper than in-context learning. *ArXiv*, abs/2205.05638, 2022. URL <https://api.semanticscholar.org/CorpusID:248693283>.
- Lu, Y., Bartolo, M., Moore, A., Riedel, S., and Stenetorp, P. Fantastically ordered prompts and where to find them: Overcoming few-shot prompt order sensitivity. *ArXiv*, abs/2104.08786, 2021. URL <https://api.semanticscholar.org/CorpusID:233296494>.
- Mao, Y., Mathias, L., Hou, R., Almahairi, A., Ma, H., Han, J., tau Yih, W., and Khabsa, M. Unipelt: A unified framework for parameter-efficient language model tuning. In *Annual Meeting of the Association for Computational Linguistics*, 2021. URL <https://api.semanticscholar.org/CorpusID:238857301>.
- Min, S., Lyu, X., Holtzman, A., Artetxe, M., Lewis, M., Hajishirzi, H., and Zettlemoyer, L. Rethinking the role of demonstrations: What makes in-context learning work? *ArXiv*, abs/2202.12837, 2022. URL <https://api.semanticscholar.org/CorpusID:247155069>.
- Pang, B. and Lee, L. A sentimental education: Sentiment analysis using subjectivity summarization based on minimum cuts. *ArXiv*, cs.CL/0409058, 2004. URL <https://api.semanticscholar.org/CorpusID:388>.
- Pang, B. and Lee, L. Seeing stars: Exploiting class relationships for sentiment categorization with respect to rating scales. In *Annual Meeting of the Association for Computational Linguistics*, 2005. URL <https://api.semanticscholar.org/CorpusID:3264224>.
- Paszke, A., Gross, S., Massa, F., Lerer, A., Bradbury, J., Chanan, G., Killeen, T., Lin, Z., Gimelshein, N., Antiga, L., Desmaison, A., Köpf, A., Yang, E., DeVito, Z., Raison, M., Tejani, A., Chilamkurthy, S., Steiner, B., Fang, L., Bai, J., and Chintala, S. Pytorch: An imperative style, high-performance deep learning library. In *Neural Information Processing Systems*, 2019.
- Phan, X. H., Nguyen, M. L., and Horiguchi, S. Learning to classify short and sparse text & web with hidden topics from large-scale data collections. In *The Web Conference*, 2008. URL <https://api.semanticscholar.org/CorpusID:16198890>.
- Radford, A., Wu, J., Child, R., Luan, D., Amodei, D., and Sutskever, I. Language models are unsupervised multitask learners. 2019.
- Rumelhart, D. E., Hinton, G. E., and Williams, R. J. Learning representations by back-propagating errors. *Nature*, 323:533–536, 1986. URL <https://api.semanticscholar.org/CorpusID:205001834>.
- Saravia, E., Liu, H.-C. T., Huang, Y.-H., Wu, J., and Chen, Y.-S. Carer: Contextualized affect representations for emotion recognition. In *Conference on Empirical Methods in Natural Language Processing*, 2018. URL <https://api.semanticscholar.org/CorpusID:53080764>.
- Socher, R., Perelygin, A., Wu, J., Chuang, J., Manning, C. D., Ng, A., and Potts, C. Recursive deep models for semantic compositionality over a sentiment treebank. In *Conference on Empirical Methods in Natural Language Processing*, 2013. URL <https://api.semanticscholar.org/CorpusID:990233>.
- Touvron, H., Lavril, T., Izacard, G., Martinet, X., Lachaux, M.-A., Lacroix, T., Rozière, B., Goyal, N., Hambro, E., Azhar, F., Rodriguez, A., Joulin, A., Grave, E., and Lample, G. Llama: Open and efficient foundation language models. *ArXiv*, abs/2302.13971, 2023. URL <https://api.semanticscholar.org/CorpusID:257219404>.
- Vaswani, A., Shazeer, N. M., Parmar, N., Uszkoreit, J., Jones, L., Gomez, A. N., Kaiser, L., and Polosukhin, I. Attention is all you need. *ArXiv*, abs/1706.03762, 2017.
- Voorhees, E. M. and Tice, D. M. Building a question answering test collection. In *Annual International ACM SIGIR Conference on Research and Development in Information Retrieval*, 2000. URL <https://api.semanticscholar.org/CorpusID:11465263>.
- Wolf, T., Debut, L., Sanh, V., Chaumond, J., Delangue, C., Moi, A., Cistac, P., Rault, T., Louf, R., Funtowicz, M., and Brew, J. Transformers: State-of-the-art natural language processing. In *Conference on Empirical Methods in Natural Language Processing*, 2019.
- Wu, X., Li, C., Aminabadi, R. Y., Yao, Z., and He, Y. Understanding int4 quantization for language models: Latency speedup, composability, and failure cases. In *International Conference on Machine Learning*, 2023. URL <https://api.semanticscholar.org/CorpusID:260550717>.
- Xu, B., Wang, Q., Mao, Z., Lyu, Y., She, Q., and Zhang, Y. knn prompting: Beyond-context learning with calibration-free nearest neighbor inference. *ArXiv*, abs/2303.13824, 2023. URL <https://api.semanticscholar.org/CorpusID:257756989>.

Zhang, A., Tay, Y., Zhang, S., Chan, A., Luu, A. T., Hui, S. C., and Fu, J. Beyond fully-connected layers with quaternions: Parameterization of hypercomplex multiplications with $1/n$ parameters. *ArXiv*, abs/2102.08597, 2021. URL <https://api.semanticscholar.org/CorpusID:231942691>.

Zhang, X., Zhao, J. J., and LeCun, Y. Character-level convolutional networks for text classification. In *Neural Information Processing Systems*, 2015. URL <https://api.semanticscholar.org/CorpusID:368182>.

Table 8. LM Performance w/ and w/o Semantic Calibration.

Dataset	Model	Clustering		Prediction			
		ARI Score \uparrow	AMI Score \uparrow	Accuracy \uparrow	Precision \uparrow	Recall \uparrow	F1 Score \uparrow
AGNews	GPT2-XL [w/o]	0.455	0.491	0.709	0.768	0.709	0.680
	GPT2-XL [w/]	0.841	0.800	0.937	0.937	0.937	0.937
	Pythia-XL [w/o]	0.237	0.394	0.641	0.794	0.641	0.656
	Pythia-XL [w/]	0.844	0.803	0.938	0.938	0.938	0.938
WebSS	GPT2-XL [w/o]	0.038	0.210	0.266	0.310	0.272	0.229
	GPT2-XL [w/]	0.618	0.643	0.813	0.836	0.799	0.809
	Pythia-XL [w/o]	0.308	0.409	0.514	0.353	0.519	0.405
	Pythia-XL [w/]	0.627	0.662	0.820	0.846	0.813	0.820

A. Implementation Details

A.1. Hyperparameters

In the demonstration selection, we randomly sample data from the training set. Following the practice of KP, we compute the maximum allowed number of demonstrations by setting the threshold of the truncation probability to be 5%. We stabilize the random number by setting the random seed as the default value of 42.

In the learning process of our approach SC, we use AdamW optimizer with a learning rate of $1e - 4$. Meanwhile, the epoch number for semantic calibration is 500 and the batch size is 1024. The learning process of the neural clustering module is separated from the LM, so we can have larger hyperparameters for semantic calibration.

In the learning process of PEFT methods, we use the same optimizer and the learning rate. For LORA and IA³, we follow the recommended practices based on their papers. That is, making the query-key-value matrices trainable in LORA, and also making the second fully-connected layer in the feed-forward module trainable in IA³. Considering the finetuning is on LMs, we take the commonly used hyperparameters, letting the epoch number be 1. The batch size is the corresponding value in pretraining LMs, that is, 512 for GPT2 models and 1024 for Pythia Models, via gradient accumulation.

In addition, we use quantization techniques (INT4) to speed up the process, with the default settings (Dettmers et al., 2023; Wu et al., 2023). It will reduce the computation costs of PEFT methods while maintaining their performance.

A.2. Environments

Our implementation uses deep learning framework PYTORCH (Paszke et al., 2019), TRANSFORMERS (Wolf et al., 2019), and use PEFT¹ to set up and conduct the parameter-efficient finetuning experiments.

The PEFT experiments are conducted on Nvidia A100 GPU (80 GB), while ICL and KP are on Nvidia V100 GPU (32 GB).

B. More Results and Analysis

B.1. Semantic Clustering

We use labels in the form of `l1m[identifier]` to mark variants, where identifier is either *w/o* or *w/*, representing whether semantic calibration is applied.

On the metrics, we use *Adjusted Rand Index (ARI)* score and *Adjusted Mutual Info (AMI)* score to measure the clustering quality. Their range is $[-1, 1]$, the larger, the better. A value close to 0 indicates a normal disordered situation. For the prediction quality, besides *Accuracy*, we also use *Precision*, *Recall*, and *F1 score*. Their range is $[0, 1]$, the larger, the better.

The results are as shown in Table 8, we can see in both prediction metrics and clustering metrics, that the semantic calibration can bring obvious improvements.

B.2. Parameter-Efficient Finetuning

Besides the recommended settings of PEFT methods, we also experimented with another setting, that is, specifying the self-attention modules in all LM layers as trainable, including the query-key-value matrices and the fully-connected projection layer. We mark them with a star symbol, such as LORA \star and IA³ \star for better distinction.

¹<https://github.com/huggingface/peft>

Table 9. Accuracy on Text Understanding with GPT2 Models.

GPT2	Method	AGNews	CARER	MR	MRPC	SST5	SUBJ	TREC	WebSS	AVG
Small	ICL	0.283	0.372	0.558	0.665	0.309	0.500	0.552	0.315	0.444
	KP	0.860	0.373	0.706	0.559	0.305	0.842	0.810	0.740	0.649
	LoRA*	0.809	0.434	0.555	0.665	0.332	0.500	0.542	0.331	0.521
	IA ³ *	0.418	0.406	0.553	0.665	0.331	0.500	0.546	0.323	0.468
	SC	0.904	0.633	0.816	0.672	0.459	0.870	0.930	0.749	0.754
Medium	ICL	0.545	0.348	0.534	0.665	0.157	0.533	0.546	0.313	0.455
	KP	0.852	0.343	0.742	0.587	0.357	0.878	0.818	0.776	0.669
	LoRA*	0.863	0.348	0.537	0.665	0.168	0.529	0.550	0.340	0.500
	IA ³ *	0.700	0.348	0.535	0.665	0.163	0.529	0.550	0.338	0.478
	SC	0.927	0.645	0.838	0.682	0.511	0.941	0.940	0.836	0.790
Large	ICL	0.684	0.441	0.793	0.665	0.286	0.617	0.622	0.208	0.539
	KP	0.854	0.394	0.847	0.597	0.375	0.895	0.882	0.763	0.701
	LoRA*	0.897	0.481	0.874	0.665	0.286	0.801	0.640	0.433	0.634
	IA ³ *	0.827	0.450	0.846	0.665	0.282	0.698	0.632	0.279	0.585
	SC	0.926	0.667	0.888	0.729	0.526	0.959	0.964	0.814	0.809
XL	ICL	0.709	0.292	0.567	0.665	0.193	0.527	0.586	0.266	0.475
	KP	0.884	0.397	0.803	0.588	0.381	0.901	0.854	0.791	0.700
	LoRA*	0.902	0.409	0.802	0.665	0.189	0.837	0.620	0.427	0.606
	IA ³ *	0.838	0.315	0.704	0.665	0.191	0.599	0.596	0.321	0.529
	SC	0.937	0.666	0.879	0.728	0.538	0.959	0.958	0.813	0.809

Table 10. Accuracy on Text Understanding with Pythia Models.

Pythia	Method	AGNews	CARER	MR	MRPC	SST5	SUBJ	TREC	WebSS	AVG
XS	ICL	0.350	0.197	0.500	0.665	0.269	0.559	0.422	0.382	0.418
	KP	0.250	0.291	0.500	0.335	0.286	0.500	0.226	0.132	0.315
	LoRA*	0.350	0.197	0.500	0.665	0.269	0.559	0.422	0.382	0.418
	IA ³ *	0.350	0.197	0.500	0.665	0.269	0.559	0.422	0.382	0.418
	SC	0.845	0.561	0.500	0.665	0.357	0.500	0.798	0.556	0.598
Small	ICL	0.517	0.342	0.548	0.665	0.239	0.524	0.360	0.181	0.422
	KP	0.250	0.291	0.500	0.335	0.286	0.500	0.226	0.132	0.315
	LoRA*	0.517	0.342	0.547	0.665	0.239	0.524	0.360	0.181	0.422
	IA ³ *	0.517	0.342	0.547	0.665	0.239	0.524	0.360	0.181	0.422
	SC	0.851	0.565	0.500	0.665	0.443	0.500	0.866	0.562	0.619
Medium	ICL	0.633	0.362	0.806	0.665	0.347	0.689	0.654	0.432	0.573
	KP	0.855	0.532	0.815	0.541	0.375	0.856	0.836	0.776	0.698
	LoRA*	0.760	0.445	0.769	0.665	0.293	0.676	0.652	0.465	0.590
	IA ³ *	0.600	0.370	0.804	0.665	0.335	0.687	0.650	0.434	0.568
	SC	0.932	0.742	0.859	0.708	0.496	0.943	0.940	0.804	0.803
Large	ICL	0.612	0.352	0.537	0.665	0.340	0.662	0.732	0.492	0.549
	KP	0.877	0.559	0.857	0.583	0.395	0.883	0.880	0.801	0.729
	LoRA*	0.891	0.589	0.838	0.665	0.420	0.863	0.754	0.497	0.690
	IA ³ *	0.797	0.396	0.571	0.665	0.346	0.736	0.744	0.493	0.593
	SC	0.936	0.751	0.888	0.734	0.489	0.951	0.962	0.822	0.816
XL	ICL	0.641	0.401	0.844	0.665	0.349	0.602	0.564	0.514	0.572
	KP	0.876	0.557	0.859	0.565	0.435	0.894	0.888	0.807	0.735
	LoRA*	0.863	0.525	0.730	0.665	0.340	0.801	0.538	0.510	0.621
	IA ³ *	0.796	0.427	0.823	0.665	0.359	0.641	0.558	0.513	0.598
	SC	0.938	0.762	0.902	0.715	0.530	0.962	0.958	0.820	0.823
XXL	ICL	0.750	0.260	0.851	0.665	0.483	0.906	0.722	0.496	0.641
	KP	0.881	0.526	0.865	0.574	0.423	0.919	0.844	0.805	0.730
	LoRA*	0.892	0.582	0.895	0.665	0.528	0.918	0.784	0.514	0.722
	IA ³ *	0.839	0.301	0.866	0.665	0.502	0.910	0.730	0.495	0.663
	SC	0.939	0.749	0.901	0.752	0.531	0.956	0.968	0.841	0.830

As shown in Table 9 and Table 10, compared with the recommended settings, LORA* performs slightly better, but still worse than KP and SC. In contrast, IA³* is slightly better on GPT2 models but slightly worse on Pythia Models.

Meanwhile, the parameter amounts of LORA* and IA³* are almost the same as LORA and IA³. It is $11 * r * d * l$ (GPT2 models) and $6 * r * d * l$ (Pythia models) for LORA*, and $8 * d * l$ (GPT2 models) and $4 * d * l$ (Pythia models) for IA³*. And also, the computation cost is similar. For example, running GPT2-XL on AGNews, SC costs 28.0 hours in forward-pass and semantic calibration, while LORA* costs 39.6 hours and IA³* costs 39.1 hours.

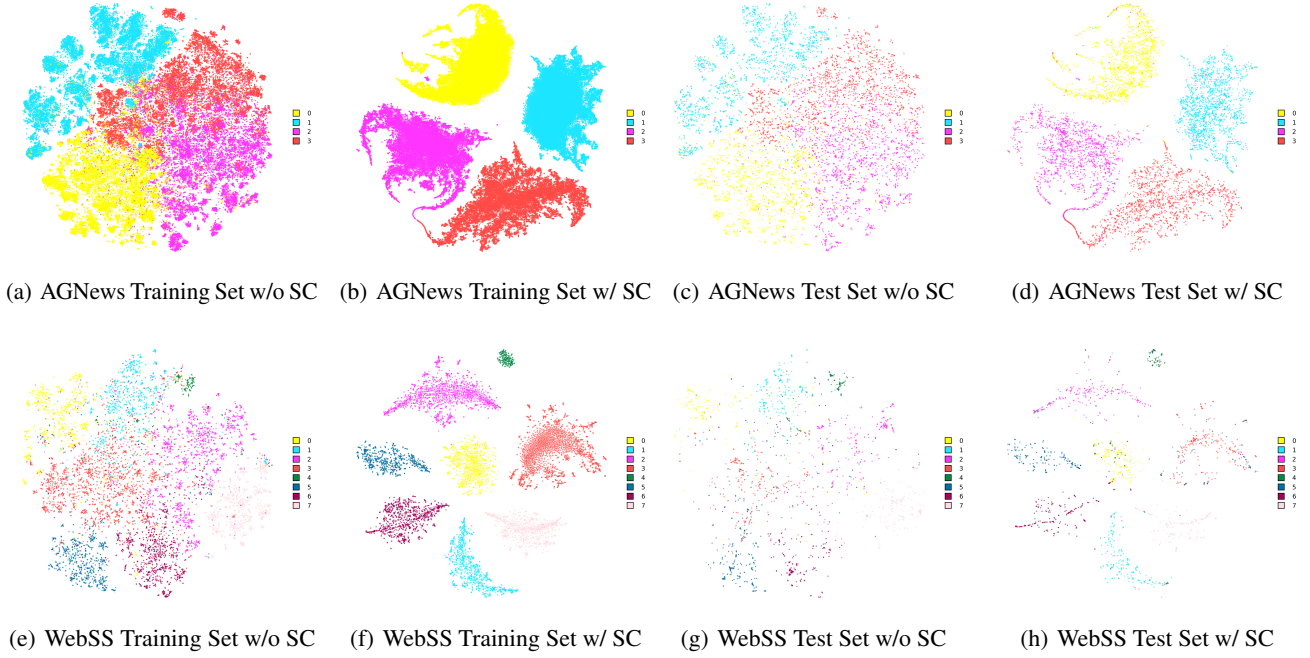


Figure 4. tSNE Illustration of Semantic Calibration in GPT2-XL Latent Space.

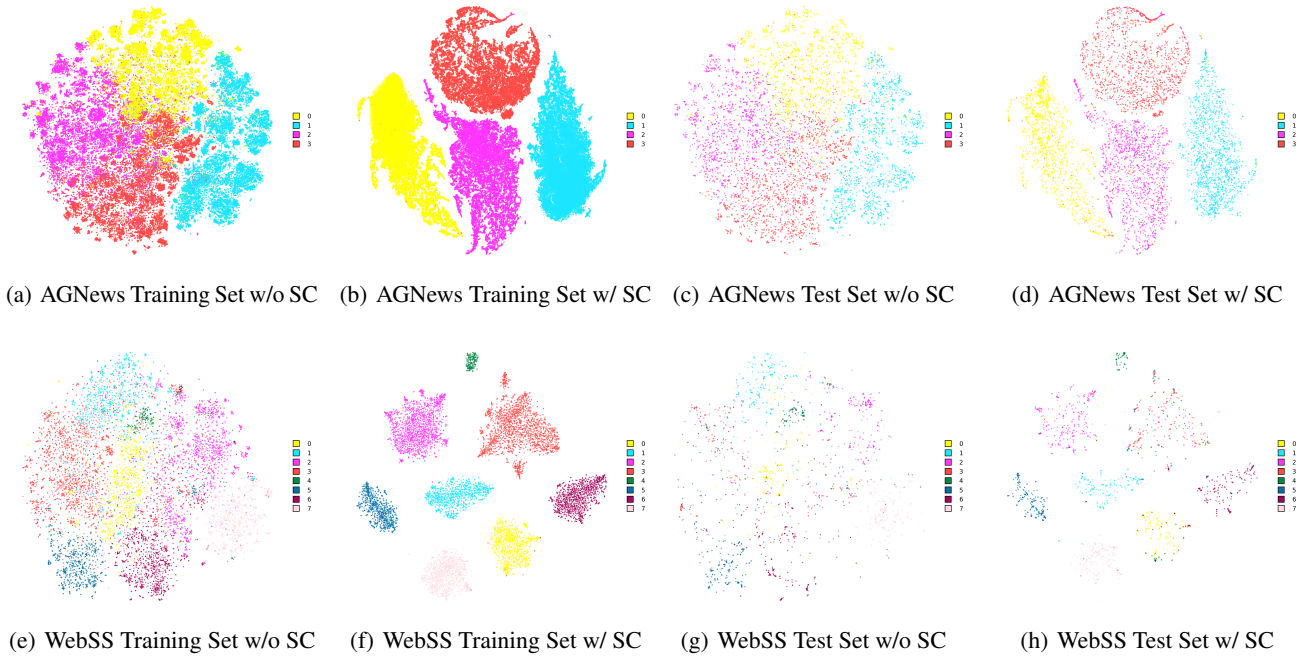


Figure 5. tSNE Illustration of Semantic Calibration in Pythia-XL Latent Space.

Table 11. Prompt Template and Label Space in the Experiments.

Dataset	Prompt	Label Space
AGNews	<i>Input:</i> Nets get Carter from Raptors. "INDIANAPOLIS – All-Star Vince Carter was traded by the Toronto Raptors to the New Jersey Nets for Alonzo Mourning, Eric Williams, Aaron Williams, and a pair of first-round draft picks yesterday." <i>Type:</i> business	world, sports, business, technology
CARER	<i>message:</i> i know a lot but i feel so stupid because i can not portray it <i>emotion:</i> sadness	sadness, joy, love, anger, fear, surprise
MR	<i>review:</i> "provides a porthole into that noble , trembling incoherence that defines us all ." <i>sentiment:</i> positive	negative, positive
MRPC	<i>Premise:</i> The 30-year bond US30YT = RR rose 22 / 32 for a yield of 4.31 percent , versus 4.35 percent at Wednesday 's close . <i>Hypothesis:</i> The 30-year bond US30YT = RR grew 1-3 / 32 for a yield of 4.30 percent , down from 4.35 percent late Wednesday . <i>Prediction:</i> equivalent	equivalent, not equivalent
SST5	<i>review:</i> a deliciously nonsensical comedy about a city coming apart at its seams . <i>sentiment:</i> great	terrible, bad, okay, good, great
SUBJ	<i>input:</i> "looking for a short cut to fame , glass concocted sources , quotes and even entire stories , but his deception did not go unnoticed forever , and eventually , his world came crumbling down . . ." <i>type:</i> objective	subjective, objective
TREC	<i>Question:</i> What currency is used in Australia ? <i>Type:</i> entity	description, entity, expression, human, location, number
WebSS	<i>input:</i> americangymnasticsclub american gymnastic club recreational gymnastics boys girls schedule fees programs calendar birthday parties camps staff <i>type:</i> sports	business, computers, culture-arts-entertainment, education-science, engineering, health, politics-society, sports

C. Representations in the Latent Space

We have more illustrations of the representations in the LM latent space, mainly on the AGNews and WebSS datasets. The illustrations on GPT2-XL are shown in Figure 4, and on Pythia-XL are shown in Figure 5.

We have findings from the illustrations. First, before and after semantic calibration, the level of data points confounding with each other is well reduced. When the label space is larger (that is, there are more classes or labels in the vocabulary), the phenomenon is more obvious. Second, semantic calibration shows a great generalization ability. The spread of data points in the test set follows the same characteristics of the corresponding training set. Third, the same data spread differently in the latent space of different models. However, the effects of semantic calibration in these latent spaces are similar.

D. Prompt Templates

The prompt templates follow the practice of prior work (Lu et al., 2021), as shown in Table 11.